BJPS

Brazilian Journal of Pharmaceutical Sciences

http://dx.doi.org/10.1590/s2175-97902024e23870

Article

Microrna-135A-5P promotes proliferation and metastasis of hepatocelluar carcinoma cells via upregulation of FOXO1

Tian Zhang[1], Lingling Guan[2], Xiaomeng Xie[2], Lixing Guo[3], Dongjing Ni[2*]

[1]Department of Pathology, Shiyan People's Hospital of Bao'an District, China, [2]Department of Gastroenterology, The Fifth Affiliated Hospital of Jinan University (Shenhe People's Hospital), China, [3]Department of Oncology, The Fifth Affiliated Hospital of Jinan University (Shenhe People's Hospital), China

Numerous studies have focused on microRNAs (miRNAs) in hepatocellular carcinoma (HCC). However, the specific role of miR-135a-5p in HCC has remained unclear. Thus, this study aimed to elucidate the role and mechanisms of action of miR-135a-5p in HCC. Transfected Huh-7 HCC cells were subjected to cell proliferation, apoptosis, migration, and invasion assays to investigate the role of miR-135a-5p and FOXO1 in modulating cellular functions. Additionally, tumor xenografts from nude mice were utilized in vivo to validate the in vitro findings. Downregulation of miR-135a-5p or upregulation of FOXO1 inhibited cell proliferation and metastasis of Huh-7 cells while promoting apoptosis. Conversely, upregulation of miR-135a-5p induced proliferation and metastasis of Huh-7 cells while suppressing apoptosis. Furthermore, FOXO1 was identified as a direct target of miR-135a-5p. Notably, downregulation of miR-135a-5p or upregulation of FOXO1 suppressed tumor growth in Huh-7 cells. Inhibition of miR-135a-5p impeded HCC cell proliferation and metastasis by upregulating FOXO1 expression.

Keywords: Hepatocellular carcinoma. MicroRNA-135a-5p. Transcription factor forkhead box O1. Proliferation. Metastasis.

INTRODUCTION

Hepatocellular carcinoma (HCC) presents a distinctive management challenge due to the high variability of its molecular phenotypes (Yang *et al.,* 2020). The incidence of HCC has been steadily rising over the past thirty years and is projected to affect over a million individuals annually by 2025 (Renne *et al.,* 2021). Hepatitis B and C viruses (HCV), host immunity, cellular mutations, and chronic inflammation are commonly believed to stimulate HCC (Zhang *et al.,* 2022). Early diagnosis allows for treatment using locoregional therapies such as surgical resection, transarterial chemoembolization, radiofrequency ablation, or liver transplantation. Nevertheless, HCC is often diagnosed at a late stage with unresectable tumors, rendering these treatments ineffective (Chidambaranathan-Reghupaty, Fisher, Sarkar, 2021). Therefore, there is an urgent need to explore novel treatment modalities for HCC.

Numerous studies have implicated microRNAs (miRNAs) in various aspects of HCC including occurrence, progression, drug resistance, and recurrence (Oura, Morishita, Masaki, 2020). Specific miRNAs such as miR-21a, miR-4262 (upregulated), and miR-98, miR-613 (downregulated) have been identified in HCC (Khan *et al.,* 2022, Xu *et al.,* 2018). Notably, miR-135a-5p-induced downregulation of tyrosine phosphatase receptor delta has been implicated as a trigger for HCV-related HCC (Van Renne *et al.,* 2018). In addition, miR-135a-5p-activated krüppel-like factor-4 (KLF4) downregulation has been

***Correspondence:** D. Ni. Department of Gastroenterology. The Fifth Affiliated Hospital of Jinan University (Shenhe People's Hospital). Jiangdong New District, Heyuan 517000, Guangdong Province, China. Phone: +86-0762-3836999. Email: Nidongjing3836@163.com. ORCID: https://orcid.org/0009-0007-7523-4820. T. Zhang: https://orcid.org/0009-0003-4091-5918. L. Guan: https://orcid.org/0009-0008-9462-5963. X. Xie: https://orcid.org/0009-0004-5294-8327. L. Guo: https://orcid.org/0009-0009-3211-0662

associated with HCC cell metastasis and proliferation via transforming growth factor-β1 (Yao *et al.,* 2016) Functional assays have revealed that exosomal miR-135a-5p stimulates HCC cell proliferation and chemotherapy resistance (Wei *et al.,* 2021). The transcription factor forkhead box O1 (FOXO1) plays a pivotal role as a tumor suppressor, involved in apoptosis, DNA damage repair, oxidative stress response, and cell cycle regulation (Reyes *et al.,* 2021). Impairment of FOXO1 has been linked to tumor stemness in HCC (Lin *et al.,* 2019), and its suppression is partially associated with HCC pathogenesis (Chand *et al.,* 2022, Yang *et al.,* 2019). Interaction between miR-135a and FOXO1 in HCC has been evidenced by miR-135a promoting HCC cell invasion through targeting FOXO1 (Zeng *et al.,* 2016). Furthermore, the miR-135a/FOXO1 axis is involved in hepatocarcinogenesis driven by hepatitis B X-interacting protein-mediated phosphoenolpyruvate carboxykinase repression (Shi *et al.,* 2016). Collectively, the molecular mechanism of miR-135a-5p and its interactions with FOXO1 warrant further investigation. Hence, this study aimed to elucidate the mechanisms of action of miR-135a-5p and FOXO1 in HCC and to identify therapeutic targets for HCC.

MATERIAL AND METHODS

Ethics statement

This study for clinical samples was approved by the ethics committee of our hospital (approval number: 20200314). The signed informed consent was obtained from the patients involved, adhering to "Good Clinical Practice". Animal experiments were reviewed and supervised by the Animal Ethics Association of our hospital (approval number: 20200722).

HCC specimen collection

Specimens were obtained from HCC patients who underwent surgical treatment at our hospital. The specimens, comprising 98 HCC tissues and 98 adjacent normal tissues (located 3 cm away from the foci) without malignant cells, were confirmed by pathology as HCC. Fresh specimens were collected during surgery, promptly frozen in liquid nitrogen, and stored at -80°C.

Among the 98 patients, 71 were male and 27 were female, with ages ranging from 24 to 73 years (median age, 51 years). Tumor differentiation grading revealed 23 cases of well-differentiated tumors and 75 cases of moderately and poorly differentiated tumors. Regarding tumor node metastasis staging, 65 cases were classified as stages I-II, and 33 cases as stages III-IV, following the standards of the International Union Against Cancer. Importantly, none of the patients had received radiotherapy or chemotherapy before undergoing surgery.

Cell culture

Human HCC cells Huh-7 (American Type Culture Collection, VA, USA) were cultured in DMEM containing 10% fet al bovine serum (FBS), 100 U/mL penicillin, and 100 U/mL streptomycin (Gibco, Grand Island, NY, USA) with 5% CO_2 at 37 □. The cells were passaged every 1-2 days, and experiments were conducted using cells in the logarithmic growth phase.

Cell grouping

The Huh-7 cells were divided into several groups, and the transfection treatments for each group are detailed in Table I. Oligonucleotides and plasmids used for transfection were sourced from GenePharma (Shanghai, China).

Huh-7 cells (2×10^5 cells/well) were seeded in a 6-well plate and cultured at 37°C with 5% CO_2. Upon 60–70% confluence, the cells were transfected according to the guidelines for Lipofectamine 2000 (Thermo Fisher Scientific, Waltham, MA, USA).

TABLE I - Transfection treatment of the cells in each group

Group	Transfection treatment
inhibitor negative control (NC) group	Huh-7 cells transfected with miR-135a-5p inhibitor negative control
miR-135a-5p inhibitor group	Huh-7 cells transfected with miR-135a-5p inhibitor
mimic NC group	Huh-7 cells transfected miR-135a-5p mimic NC
miR-135a-5p mimic group	Huh-7 cells transfected with miR-135a-5p mimic
overexpression NC group	Huh-7 cells transfected with pcDNA empty vector
FOXO1 overexpression group	Huh-7 cells transfected with pcDNA-FOXO1 vector
miR-135a-5p inhibitor + siRNA-FOXO1 group	Huh-7 cells transfected with miR-135a-5p inhibitor and FOXO1 siRNA

Note: inhibitor negative control (NC) group is named as Inhibitor-Ctrl; miR-135a-5p inhibitor group is named as miR-135a-5p inhibitor; mimic NC group is named as mimic-Ctrl; miR-135a-5p mimic group is named as miR-135a-5p mimic; overexpression NC group is named as Oe-Ctrl; FOXO1 overexpression group is named as Oe-FOXO1; miR-135a-5p inhibitor + siRNA-FOXO1 group is named as miR-135a-5p inhibitor + si-FOXO1.

RT-qPCR

Total RNA was extracted from tissues and cells using TRIzol reagent (Invitrogen, Carlsbad, California, USA). For FOXO1, RT-qPCR was performed using the PrimeScript RT Reagent Kit (Takara) and SYBR Premix Ex Taq II (Takara). GAPDH served as the endogenous control. For miR-135a-5p, the Mir-X miR First-Strand Synthesis Kit (Takara) and SYBR Premix Ex Taq II (Takara) were utilized for RT-qPCR, with U6 used as a loading control. The thermocycling conditions were as follows: initial denaturation for 30 s at 95 °C, followed by 40 cycles of denaturation for 5 s at 95 °C, annealing for 30 s at 55 °C, and extension for 30 s at 72 °C. Primer sequences were designed and synthesized by BGI Tech (Beijing, China) (Table II). Subsequently, the melting curve was analyzed, and data were analyzed using the $2^{-\Delta\Delta Ct}$ method.

TABLE II - Primer sequence in this study

Gene	Primer sequence (5'-3')
miR-135a-5p	Forward: 5'-TATGGCTTTTTATTCCTATGTGA-3'
	Reverse: Universal primer
FOXO1	Forward: 5'-GCTGCATCCATGGACAACAACA-3'
	Reverse: 5'-CGAGGGCGAAATGTACTCCAGTT-3'
U6	Forward: 5'-CTCGCTTCGGCAGCACATATACT-3'
	Reverse: 5'-ACGCTTCACGAATTTGCGTGTC-3'
GAPDH	Forward: 5'-TCAACGACCACTTTGTCAAGCTCA-3'
	Reverse: 5'-GCTGGTGGTCCAGGGGTCTTACT-3'

Note: miR-135a-5p, microRNA-135a-5p; FOXO1, Transcription factor forkhead box O1; GAPDH, glyceraldehyde-3-phosphate dehydrogenase.

Western blot analysis

Protein extraction was performed using RIPA lysis buffer containing a protease inhibitor (Boster, Wuhan, China), and quantification was carried out using the bicinchoninic acid method. The proteins were then separated by sodium dodecyl sulfate-polyacrylamide gel electrophoresis and transferred onto a polyvinylidene fluoride (PVDF) membrane. Subsequently, the PVDF membrane was blocked with a blocking solution containing 5% non-fat dry milk in PBST at room temperature for 1 hour. Primary antibodies FOXO1 (1:1000) and GAPDH (1:1000, Cell Signaling Technologies, Danvers, MA, USA) were applied overnight at 4 °C, followed by probing with the secondary antibody (1:5000, Cell Signaling Technologies) for 1 h at room temperature. Subsequently, enhanced chemiluminescence was added to the membrane for development, followed by exposure and photography. The resulting image was quantified using a gel image processing system (Quantity One), with GAPDH serving as the control. Protein expression levels of the target genes were determined as the ratio of the gray values.

Cell viability assay

The culture medium was discarded at 24, 48, and 72 h post-transfection. The cells were incubated with 100 µL of serum-free DMEM and 10 µL of CCK-8 solution (Dojindo Laboratories, Kumamoto,Japan) in darkness. After 2 h of incubation, the optical density (OD) was measured at 450 nm using a microplate reader.

Apoptosis by flow cytometry

Annexin V-fluorescein isothiocyanate (FITC)/ propidium iodide (PI) double staining and flow cytometry were performed to detect apoptosis. The cells were washed in phosphate-buffered saline (PBS) and resuspended in 200 µl binding buffer, followed by incubation with 5 µL of Annexin V-FITC and staining with 10 µL of PI solution. Subsequently, cell apoptosis was measured using a flow cytometer within 30 minutes. For result interpretation, Annexin V was plotted on the abscissa axis and PI on the vertical axis. The upper left quadrant indicated (Annexin V-FITC)-/PI+, signifying necrotic cells; the upper right quadrant denoted (Annexin V-FITC)+/PI+, revealing late-apoptotic cells; the lower right quadrant referred to (Annexin V-FITC)+/PI-, demonstrating early-apoptotic cells; while the lower left quadrant represented (Annexin V-FITC)-/PI-, indicating living cells. The apoptotic rate of cells was estimated as the percentage of late apoptotic cells, combined with the proportion of early apoptotic cells.

Cell invasion and migration assay

The cell invasion assay was implemented using Matrigel® (BD Biosciences, Franklin Lakes, NJ, USA)-coated Transwell chambers with an 8-µm pore polycarbonate membrane (Costar; Corning Incorporated, Corning, NY, USA) following the manufacturer's instructions. Transfected cells were resuspended in FBS-free medium at a density of 2×10^4 cells/mL. The upper chamber was filled with 500 µL of the cell suspension, while the lower chamber contained medium with 10% FBS as the chemoattractant. Following a 48-hour incubation period, cells that had successfully invaded were fixed with 4% paraformaldehyde, stained with 0.1% crystal violet, and enumerated under a light microscope. In the cell migration experiment, the upper chamber of the Transwell chamber was devoid of the Matrigel coating, while the remaining procedures were identical to those in the invasion experiment.

Tumor xenografts in nude mice

A total of 24 male BALB/c nude mice were randomly divided into four groups (n = 6): inhibitor-Ctrl, miR-135a-5p inhibitor, Oe-Ctrl, and Oe-FOXO1.

Cells in each group were detached and collected in centrifuge tubes to obtain cell suspensions (1×10^7 cells/mL) in PBS. Nude mice were disinfected routinely and injected with 0.2 mL of a single cell suspension subcutaneously into the armpit of the right forelimb. Following injection, the nude mice were kept under specific pathogen-free (SPF) conditions, and the formation of subcutaneous tumors was monitored continuously. On the 21st day post-injection, the nude mice were euthanized via carbon dioxide asphyxiation, and tumors were harvested. Tumors were measured using

a Vernier caliper, weighed using an electronic balance, and photographed. Tumor volume was calculated using the formula: (a) × width $(b)^2/2$. Subsequently, the nude mice were euthanized, and the graft tumors were excised, collected, and fixed with 4% paraformaldehyde for 24 h. Following fixation, they underwent xylene and gradient alcohol dehydration, embedding in paraffin, and routine sectioning into 4 μm thickness for immunohistochemical staining, following the methodology described in the reference (Lu *et al.,* 2018).

Dual luciferase reporter gene assay

The putative binding site of the 3'-untranslated region (UTR) of FOXO1 and miR-135a-5p was cloned into the pGL3 luciferase vector (Promega, Madison, WI, United States) to obtain FOXO1 wild type (Wt), and the binding site was mutated and then cloned into the pGL3 luciferase vector to obtain FOXO1 mutant (Mut). Huh-7 cells were seeded in a 24-well plate and co-transfected with FOXO1-Wt or FOXO1-Mut and miR-135a-5p mimic or mimic NC using Lipofectamine 2000 (Thermo Fisher Scientific). The corresponding luciferase activity was detected 48 h later using the manufacturer's instructions (Promega Corporation, Madison, WI, USA).

Statistical analysis

All data were analyzed using Statistical software (IBM Corp. Armonk, NY, USA). Normal distribution of the observed data was confirmed using the Shapiro-Wilk W test, and results are presented as mean ± standard deviation. Differences between groups were assessed using unpaired (independent samples) or paired samples (paired data) with Student's t-test or one-way analysis of variance (ANOVA), followed by Tukey's post hoc test for multiple comparisons, where appropriate. Correlation analysis was conducted using Pearson's test. A significance level of $P < 0.05$ was considered statistically significant.

RESULTS

MiR-135a-5p is highly expressed and FOXO1 is poorly expressed in HCC tissues

The expression levels of miR-135a-5p and FOXO1 were assessed in HCC tissues and adjacent normal tissues using RT-qPCR and western blot analyses (Figure 1A-D). Compared to adjacent normal tissues, miR-135a-5p expression was elevated while FOXO1 expression was reduced in HCC tissues ($P < 0.05$). Further analysis using Pearson's correlation revealed a negative correlation between the expression of miR-135a-5p and FOXO1 in HCC tissues ($P < 0.05$) (Figure 1E). Additionally, miR-135a-5p expression exhibited significant associations with TNM stage and tumor differentiation ($P < 0.05$), but not with the age and sex of HCC patients ($P > 0.05$) (Figure 1F-I).

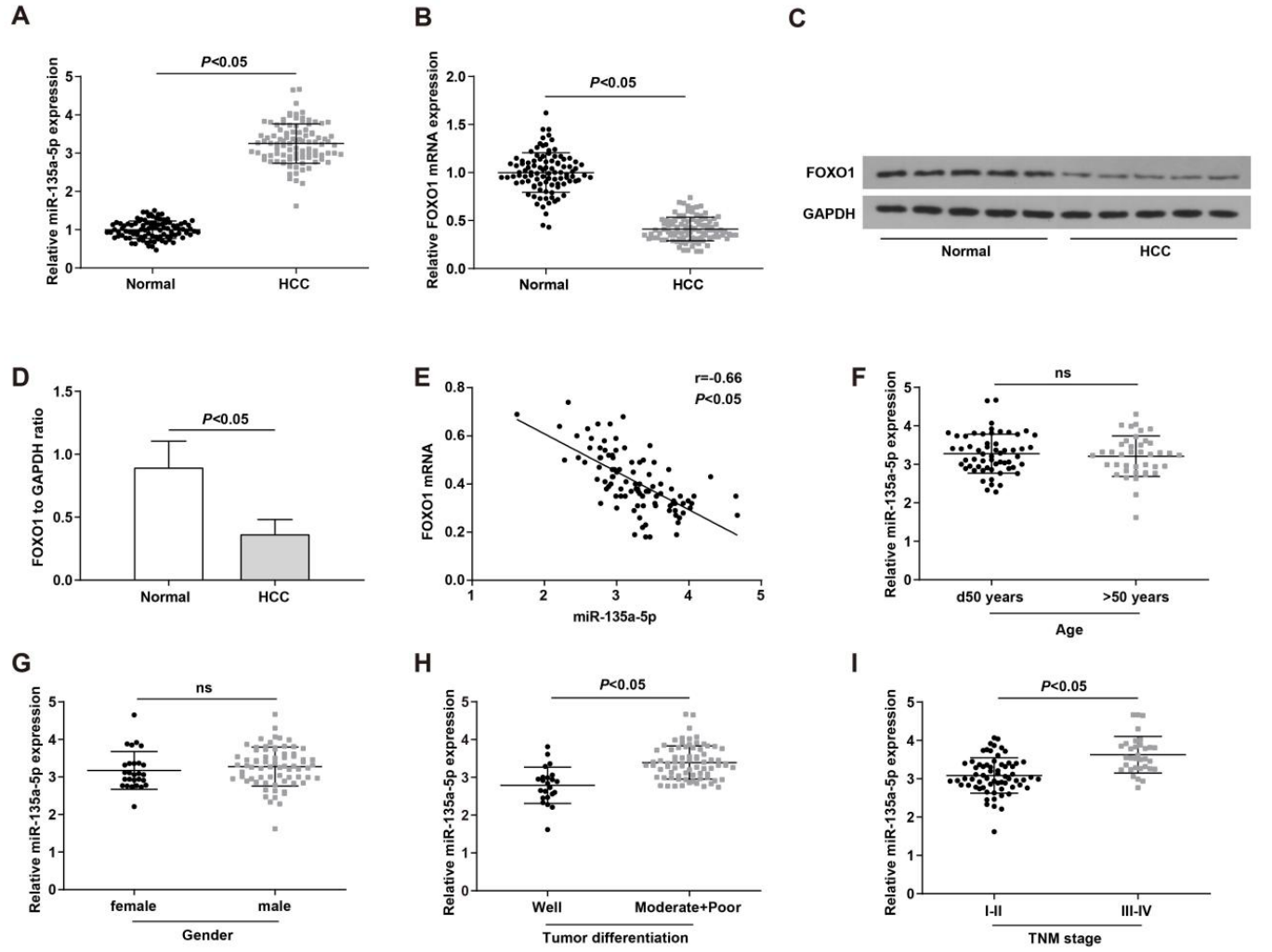

FIGURE 1 - MiR-135a-5p is highly expressed and FOXO1 is poorly expressed in HCC tissues. A. MiR-135a-5p expression in HCC tissues (n = 98) and adjacent normal tissues (n = 98); B. FOXO1 mRNA expression in HCC tissues (n = 98) and adjacent normal tissues (n = 98); C-D. FOXO1 protein expression in HCC tissues (n = 98) and adjacent normal tissues (n = 98); E. The correlation between miR-135a-5p and FOXO1 mRNA expression in patients with HCC (n = 98). F-I. Correlation between miR-135a-5p expression and the clinicopathologic features of HCC patients.

miR-135a-5p targets FOXO1 expression in HCC cells

Two publicly available algorithms, DIANA TOOLS and TargetScan, were utilized to identify potential targets of miR-135a-5p. TargetScan predicted FOXO1 as a potential target of miR-135a-5p (Figure 2A). Based on the predicted binding sites of miR-135a-5p, luciferase reporter plasmids containing FOXO1 3' untranslated region (3'UTR) wild type (Wt) and mutant type (Mut) were generated (Figure 2B). A luciferase reporter assay was performed by co-transfecting the luciferase reporter plasmids with either the miR-135a-5p mimic or its control. As depicted in Figure 2C, the overexpression of miR-135a-5p resulted in decreased luciferase activity driven by the Wt 3'UTR of FOXO1 ($P < 0.05$), while no significant alteration in luciferase activity driven by the Mut 3'UTR of FOXO1 was observed ($P > 0.05$).

Furthermore, the expression levels of miR-135a-5p and FOXO1 were detected in Huh-7 cells using RT-qPCR and western blot analysis (Figure 2D-F). In the miR-135a-5p mimic group, miR-135a-5p expression was upregulated compared to the NC group, while it was downregulated in the miR-135a-5p inhibitor group ($P < 0.05$). Correspondingly, the expression of

FOXO1 was significantly decreased in the miR-135a-5p mimic group and increased in the miR-135a-5p inhibitor group compared to the NC group ($P < 0.05$). Moreover, FOXO1 expression was notably elevated in the Oe-FOXO1 group compared to the Oe-Ctrl group ($P < 0.05$). Conversely, in the miR-135a-5p inhibitor group, FOXO1 expression was significantly reduced in the miR-135a-5p inhibitor + si-FOXO1 group ($P < 0.05$). These findings indicate that miR-135a-5p targets FOXO1 and inhibits its expression.

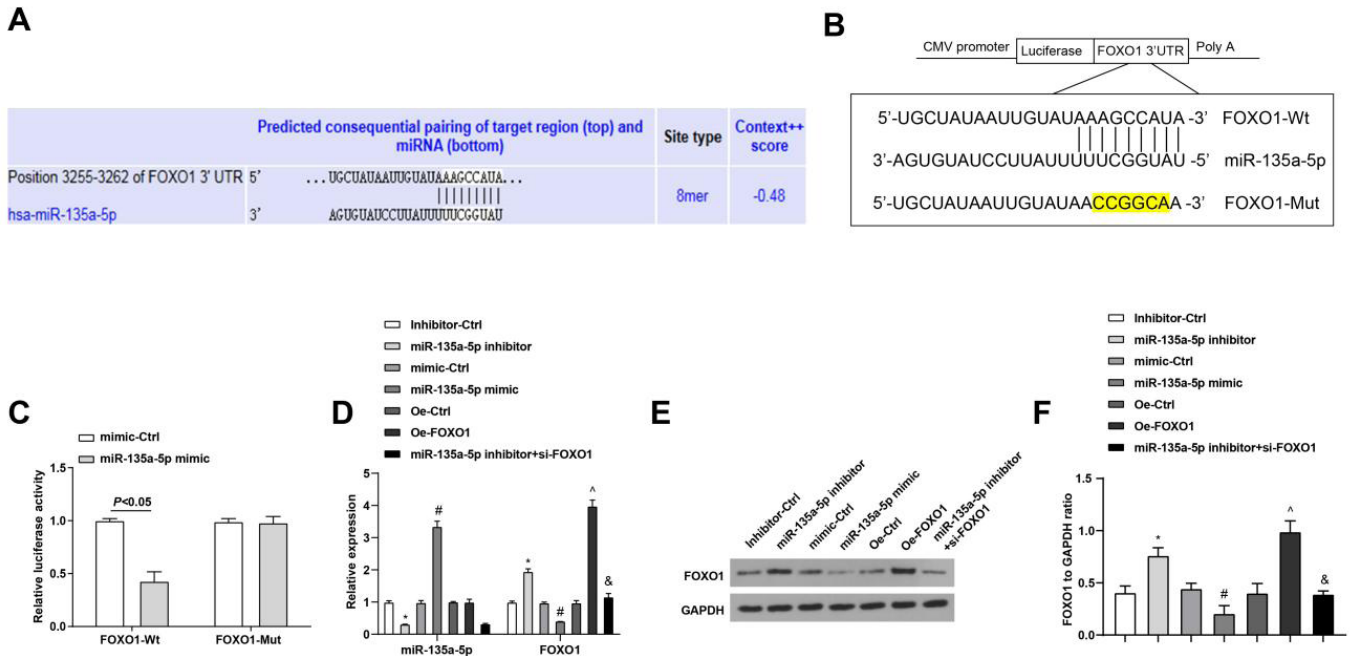

FIGURE 2 - miR-135a-5p targets FOXO1 expression in HCC cells. A. Predicted consequential pairing of the target region (FOXO1 3'UTR) and miR-135a-5p from TargetScan (http://www.targetscan.org/vert_72/); B. Schematic illustration of the predicted miR-135a-5p binding sites with the 3'UTR of FOXO1; C. Luciferase activity assay was performed in Huh-7 cells co-transfected with miR-135a-5p and the luciferase reporter plasmids driven by either Wt or Mut 3'UTR of FOXO1; D. miR-135a-5p and FOXO1 mRNA expression in Huh-7 cells; E-F. FOXO1 protein expression in Huh-7 cells; * $P < 0.05$ compared with the Inhibitor-Ctrl group; # $P < 0.05$ compared with the mimic-Ctrl group; ^ $P < 0.05$ compared with the Oe-Ctrl group; & $P < 0.05$ compared with the miR-135a-5p inhibitor group.

miR-135a-5p modulates FOXO1 to affect HCC cell proliferation and apoptosis

The proliferation of Huh-7 cells in each group was assessed using the CCK-8 assay (Figure 3A). Cell proliferation was significantly inhibited in the miR-135a-5p inhibitor and Oe-FOXO1 groups compared to the inhibitor-Ctrl and Oe-Ctrl groups (both $P < 0.05$). Conversely, cell proliferation was enhanced in the miR-135a-5p mimic group compared to the mimic-Ctrl group ($P < 0.05$). Additionally, cell proliferation was further increased in the miR-135a-5p inhibitor + si-FOXO1 group compared to the miR-135a-5p inhibitor group (all $P < 0.05$).

Cell apoptosis was assessed using Annexin V-FITC/PI double staining (Figure 3B,C). The results demonstrated that the apoptosis rate was significantly elevated in the miR-135a-5p inhibitor and Oe-FOXO1 groups compared to the inhibitor-Ctrl and Oe-Ctrl groups (both $P < 0.05$). Conversely, the rate of apoptosis was reduced in the miR-135a-5p mimic group compared to the mimic-Ctrl group ($P < 0.05$). Moreover, the apoptosis rate was lower in the miR-135a-5p inhibitor + si-FOXO1 group compared to the miR-135a-5p inhibitor group ($P < 0.05$).

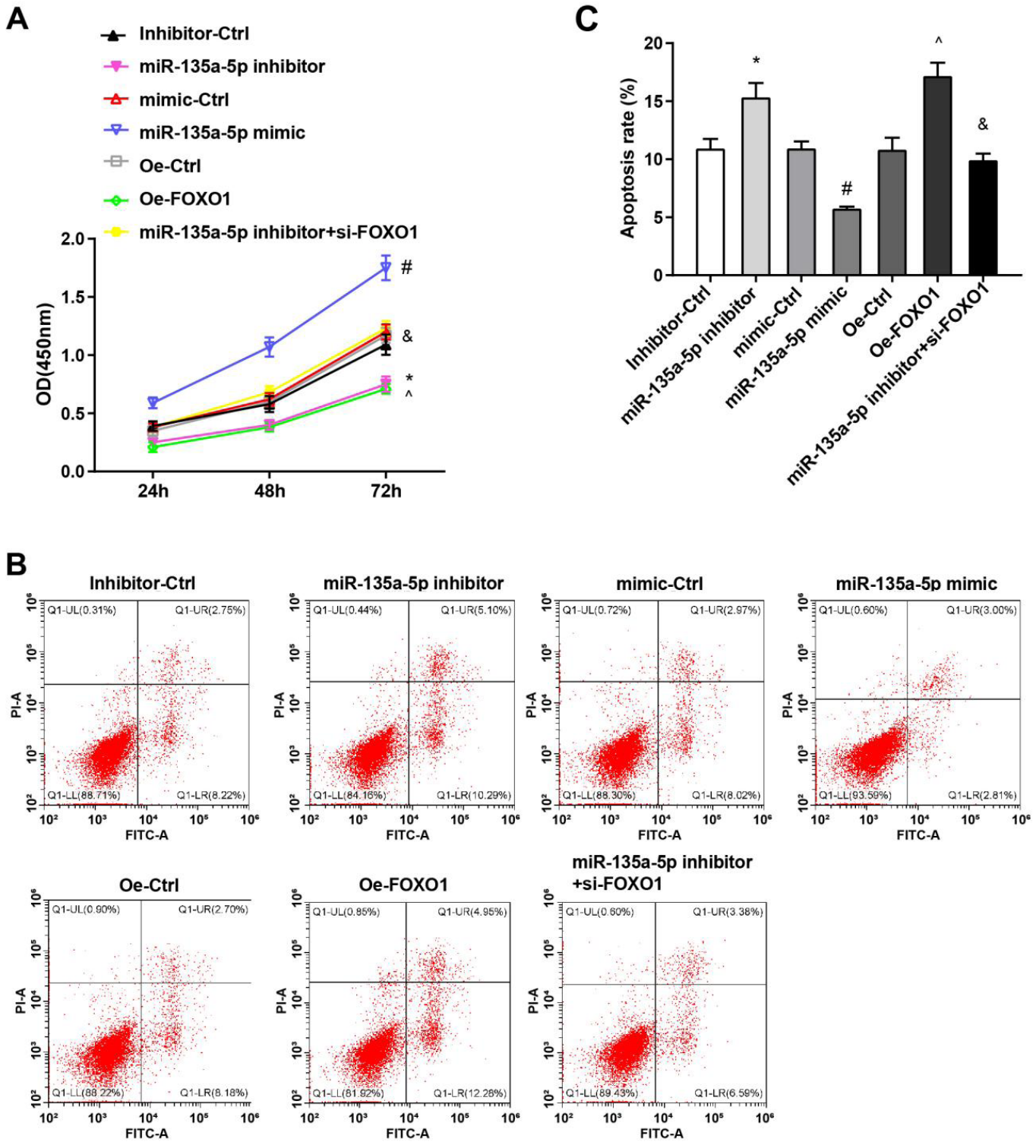

FIGURE 3 - miR-135a-5p modulates FOXO1 to impact HCC cell proliferation and apoptosis. A. CCK-8 detection of the growth curve of Huh-7 cells in each group; B. Flow cytometry of Huh-7 cell apoptosis; C. Huh-7 cell apoptosis rate; * $P < 0.05$ compared with the Inhibitor-Ctrl group; # $P < 0.05$ compared with the mimic-Ctrl group; ^ $P < 0.05$ compared with the Oe-Ctrl group; & $P < 0.05$ compared with the miR-135a-5p inhibitor group.

miR-135a-5p modulates FOXO1 to affect HCC cell invasion and migration

A transwell assay was employed to detect the migration and invasion abilities of Huh-7 cells in each group (Figure 4A-D). Compared to the Inhibitor-Ctrl and Oe-Ctrl groups, both the miR-135a-5p inhibitor and Oe-FOXO1 groups exhibited suppressed cell migration and invasion abilities (both $P < 0.05$). Conversely, the miR-135a-5p mimic group showed enhanced cell migration and invasion abilities compared to the mimic-Ctrl group ($P < 0.05$). Moreover, compared to the miR-135a-5p inhibitor group, the miR-135a-5p inhibitor + si-FOXO1 group displayed increased cell migration and invasion abilities ($P < 0.05$).

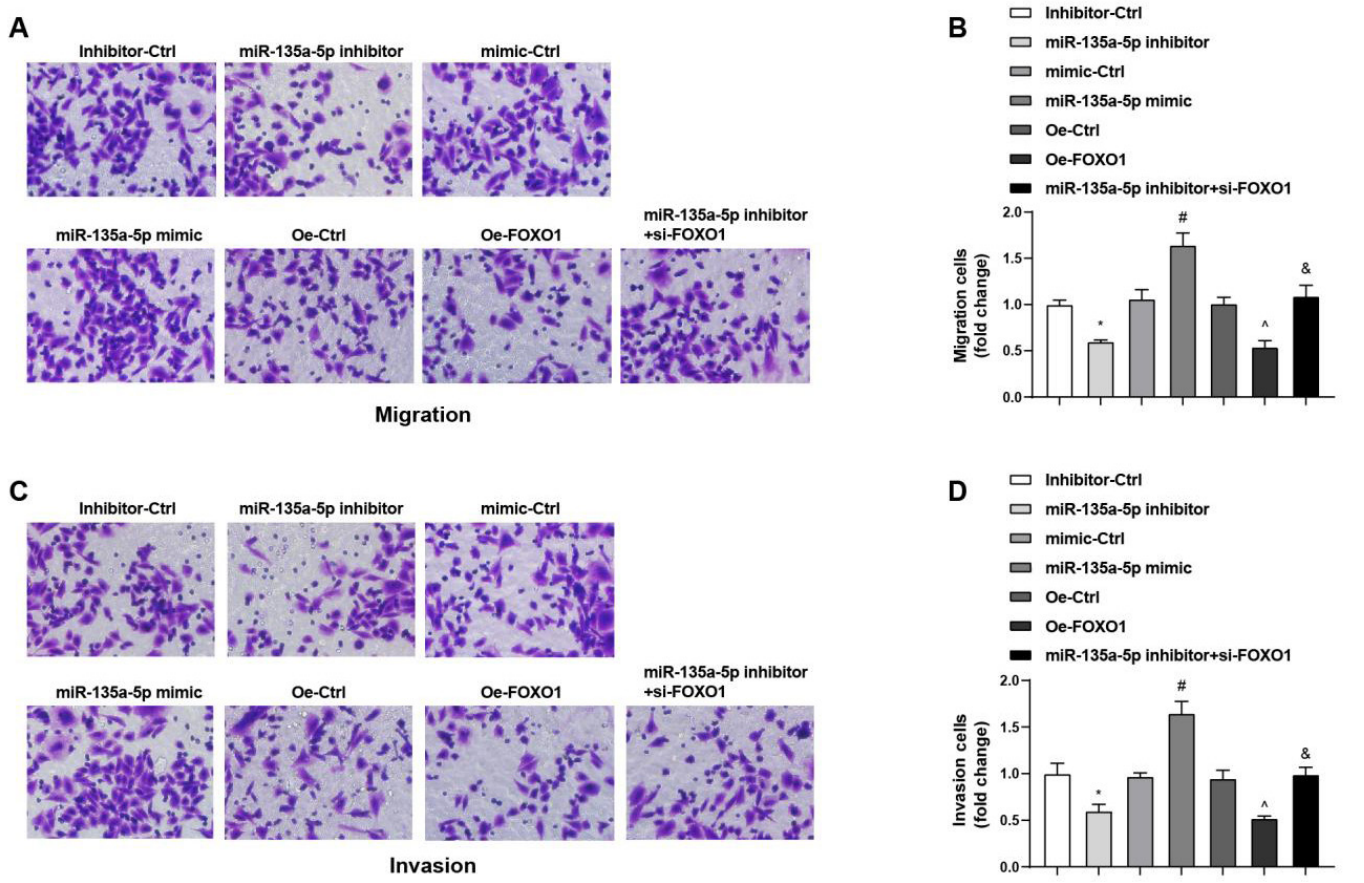

FIGURE 4 - miR-135a-5p modulates FOXO1 to impact HCC cell invasion and migration. A-B. Transwell detection of migration ability of Huh-7 cells; C-D. Transwell detection of invasion ability of Huh-7 cells; * $P < 0.05$ compared with the Inhibitor-Ctrl group; # $P < 0.05$ compared with the mimic-Ctrl group; ^ $P < 0.05$ compared with the Oe-Ctrl group; & $P < 0.05$ compared with the miR-135a-5p inhibitor group.

miR-135a-5p downregulation and FOXO1 upregulation retard tumor growth in nude mice with HCC

In vivo xenografting of Huh-7 cells into nude mice was conducted to evaluate tumor growth status. The results revealed that (Figure 5A-C), compared to the Inhibitor-Ctrl and Oe-Ctrl groups, both tumor volume and weight were decreased in the miR-135a-5p inhibitor and Oe-FOXO1 groups (both $P < 0.05$). Immunohistochemistry was utilized to assess Ki-67 expression levels. The analysis demonstrated that Ki-67 expression levels were reduced in the miR-135a-5p inhibitor and Oe-FOXO1 groups compared to the Inhibitor-Ctrl and Oe-Ctrl groups (both $P < 0.05$) (Figure 5D).

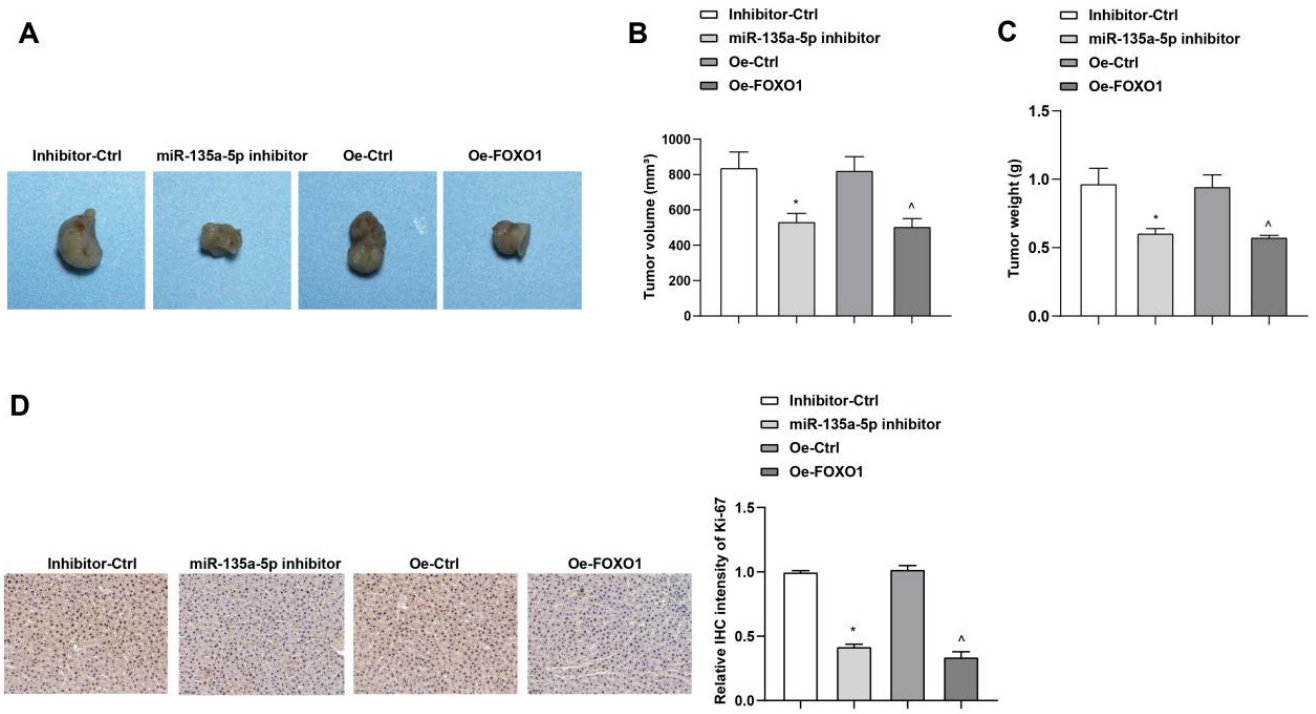

FIGURE 5 - miR-135a-5p downregulation and FOXO1 upregulation retard tumor growth in nude mice with HCC. A. Tumors in nude mice; B. Tumor volume of nude mice; C. Tumor weight of nude mice; D. Ki-67 expression levels were determined by immunohistochemistry. * $P < 0.05$ compared with the Inhibitor-Ctrl group; ^ $P < 0.05$ compared with the Oe-Ctrl group.

DISCUSSION

HCC is one of the predominant causes of cancer-related deaths and is the primary cause of death among patients with cirrhosis (Sidali *et al.,* 2022). MiR-135a-5p is a crucial regulator of HCC (Lin *et al.,* 2022). However, further investigation is warranted into the miR-135a-5p/FOXO1 regulatory axis in HCC. This study was initiated to elucidate the mechanisms involving miR-135a-5p and FOXO1 in HCC and to conclude that downregulation of miR-135a-5p hampers HCC cell proliferation and metastasis by upregulating FOXO1 expression (Figure 6).

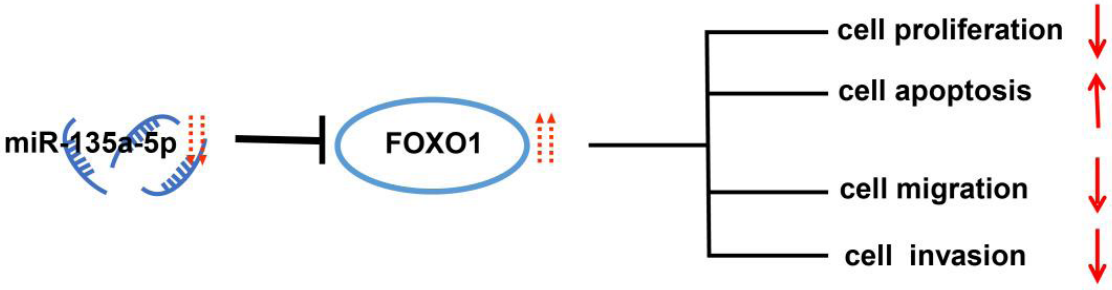

FIGURE 6 - The molecular mechanism involved in miR-135a-5p targets FOXO1 for HCC development.

Initially, we assessed the expression levels of miR-135a-5p and FOXO1 in HCC tissues, revealing elevated miR-135a-5p expression and decreased FOXO1 expression. Consistent with our observations, a previous

study reported heightened miR-135a-5p expression in HCC tissues (Yao *et al*., 2016). Additionally, miR-135a expression is upregulated in HCC tissues, correlating with tumor staging, microvascular invasion, recurrence, and poor survival outcomes (Huang *et al.,* 2017). In addition, miR-135a-5p expression is increased in HCC tissues compared to adjacent non-cancerous tissues (Wei *et al.,* 2021). Our findings also revealed a close association between miR-135a-5p expression and TNM stage and tumor differentiation, consistent with previous reports linking miR-135a expression to tumor staging, recurrence, and reduced disease-free survival in HCC (Huang *et al*., 2017). Another study highlighted that tumors with elevated miR-135a expression exhibit more aggressive characteristics than those with low levels (Yan *et al*., 2016). All these studies validated the tumor-promoting effect of miR-135a-5p in HCC, suggesting a link between miR-135a-5p and malignant behavior, thereby highlighting its potential use as a therapeutic target. FOXO1 expression is exhibited that lower FOXO1 expression appears in HCC tissues and cells (Wang *et al.,* 2019). Other articles have also indicated poorly expressed FOXO1 in HCC tissues and cells (Hu *et al.,* 2022, Yang *et al.,* 2019). These studies have validated the tumor-suppressive effect of FOXO1 in HCC. Nevertheless, the results of the present study are in agreement with these findings.

To explore the role of miR-135a-5p and FOXO1 in HCC cell progression, a series of assays were performed, demonstrating that downregulation of miR-135a-5p or upregulation of FOXO1 impeded HCC proliferation and metastasis while promoting cell apoptosis. Conversely, upregulation of miR-135a-5p induced HCC cell proliferation and metastasis while suppressing cell apoptosis. These findings underscore the critical roles of miR-135a-5p and FOXO1 in modulating HCC progression. Previous research has indicated a strong positive correlation between miR-135a expression and malignant behavior in HCC, suggesting its potential utility as a prognostic marker and therapeutic target (Huang *et al.,* 2017). Functional assays have revealed that exosomal miR-135a-5p stimulates apoptosis, cell proliferation, and chemotherapy resistance in HCC (Wei *et al.,* 2021). The roles of FOXO proteins, particularly FOXO1, in HCC have established a theoretical foundation for potential targeted treatment of HCC (Yang *et al.,* 2021). The upregulation of FOXO1 is partially involved in the inhibition of HCC cell proliferation and apoptosis stimulation (Wang *et al.,* 2019). Additionally, it has been previously documented that upregulation of FOXO impedes HCC cell viability and promotes cell apoptosis, and the influence of the miR-142-5p inhibitor on HCC cell viability and apoptosis is counteracted by the elevation of FOXO (Lou *et al.,* 2017). FOXO1 inhibits hepatocarcinoma growth based on gain- and loss-of-function studies, and miR-9-5p/FOXO1/CPEB3 FFL promotes HCC cell growth and tumor progression both in animal and cellular assays (Hu *et al.,* 2022). These findings are consistent with the results of the present study.

Subsequently, we identified FOXO1 as a direct target gene of miR-135a-5p. Consistent with our findings, previous studies have confirmed the targeting relationship between miR-135a-5p and FOXO1 in other diseases; FOXO1 has been validated as a target of miR-135a-5p, with miR-135a-5p negatively modulating FOXO1 expression (Wei *et al*., 2020; Xu *et al*., 2020). Additionally, there are publications demonstrating the targeting relationship between miR-135a and FOXO1, whereby miR-135a reduces FOXO1 expression by directly targeting the FOXO1 3'UTR (Shi *et al.,* 2016; Zeng *et al*., 2016). In our study, rescue experiments revealed that downregulation of FOXO1 reversed the effects of downregulated miR-135a-5p on the malignant behavior of HCC. To further validate the roles of reduced miR-135a-5p and elevated FOXO1 in HCC, we conducted tumor xenograft experiments in nude mice in vivo. The results demonstrated that reduced miR-135a-5p or elevated FOXO1 impeded tumor growth in nude mice. Previous research has confirmed that miR-135a inhibition interferes with tumor growth in bladder cancer (Li et al., 2018), and the blockade of miR-135a-5p inhibits HCC tumor proliferation and metastasis in vivo (Yao *et al*., 2016). Additionally, nude mice with HCC have been shown to suppress tumor growth upon FOXO1 overexpression (Wang *et al*., 2019), and smaller xenograft tumors have been observed in nude mice injected with FOXO1 (Yang *et al.,* 2019).

Furthermore, it is worth noting that miR-135a comprises both miR-135a-3p and miR-135a-5p, and we specifically focused on miR-135a-5p for its relevance

in our study. Previous research has indicated that miR-135a promotes HCC cell migration and invasion, with a potential mechanism involving the suppression of FOXO1 (Zeng *et al*., 2016). Their study shed light on the crucial role of miR-135a in HCC and suggested the involvement of FOXO1 in its mechanism of action. However, our study took a more comprehensive approach by conducting assays on transfected HCC cell line Huh-7 cells to investigate the roles of both miR-135a-5p and FOXO1 in modulating cellular functions, including proliferation, apoptosis, migration, and invasion. Additionally, we employed tumor xenografts from nude mice in vivo to further validate the in vitro results. Our study underscores the significant contributions of both miR-135a and FOXO in HCC progression, with these effects also confirmed in animal experiments, representing the innovation of our study.

In summary, this study demonstrated that the inhibition of miR-135a-5p impedes HCC cell proliferation and metastasis through upregulation of FOXO1. These findings highlight the substantial role of the miR-135a-5p/FOXO1 regulatory axis in HCC and suggest a potential molecular therapeutic target for the disease. Nonetheless, larger cohort studies are warranted to explore novel therapies for HCC.

REFERENCES

Chand V, Liao X, Guzman G, Benevolenskaya E, Raychaudhuri P. Hepatocellular carcinoma evades RB1-induced senescence by activating the FOXM1-FOXO1 axis. Oncogene. 2022;41(30):3778-3790.

Chidambaranathan-Reghupaty S, Fisher PB, Sarkar D. Hepatocellular carcinoma (HCC): Epidemiology, etiology and molecular classification. Adv Cancer Res. 2021;149:1-61.

Hu H, Huang W, Zhang H, Li J, Zhang Q, Miao Y R, et al. A miR-9-5p/FOXO1/CPEB3 Feed-Forward Loop Drives the Progression of Hepatocellular Carcinoma. Cells. 2022;11(13).

Huang KT, Kuo IY, Tsai MC, Wu CH, Hsu LW, Chen LY, et al. Factor VII-Induced MicroRNA-135a Inhibits Autophagy and Is Associated with Poor Prognosis in Hepatocellular Carcinoma. Mol Ther Nucleic Acids. 2017;9:274-283.

Khan S, Zhang DY, Zhang JY, Hayat MK, Ren J, Nasir S, et al. The Key Role of microRNAs in Initiation and Progression of Hepatocellular Carcinoma. Front Oncol. 2022;12:950374.

Li P, Yang X, Yuan W, Yang C, Zhang X, Han J, et al. CircRNA-Cdr1as Exerts Anti-Oncogenic Functions in Bladder Cancer by Sponging MicroRNA-135a. Cell Physiol Biochem. 2018;46(4):1606-1616.

Lin J, Lian X, Xue S, Ouyang L, Zhou L, Lu Y, et al. HBV Promotes the Proliferation of Liver Cancer Cells through the hsa_circ_0000847/miR-135a Pathway. Evid Based Complement Alternat Med. 2022;2022:7332337.

Lin X, Zuo S, Luo R, Li Y, Yu G, Zou Y, et al. HBX-induced miR-5188 impairs FOXO1 to stimulate beta-catenin nuclear translocation and promotes tumor stemness in hepatocellular carcinoma. Theranostics. 2019;9(25):7583-7598.

Lou K, Chen N, Li Z, Zhang B, Wang X, Chen Y, et al. MicroRNA-142-5p Overexpression Inhibits Cell Growth and Induces Apoptosis by Regulating FOXO in Hepatocellular Carcinoma Cells. Oncol Res. 2017;25(1):65-73.

Lu YX, Wu QN, Chen DL, Chen LZ, Wang ZX, Ren C, et al. Pharmacological Ascorbate Suppresses Growth of Gastric Cancer Cells with GLUT1 Overexpression and Enhances the Efficacy of Oxaliplatin Through Redox Modulation. Theranostics. 2018;8(5):1312-1326.

Oura K, Morishita A, Masaki T. Molecular and Functional Roles of MicroRNAs in the Progression of Hepatocellular Carcinoma-A Review. Int J Mol Sci. 2020;21(21).

Renne SL, Sarcognato S, Sacchi D, Guido M, Roncalli M, Terracciano L, et al. Hepatocellular carcinoma: a clinical and pathological overview. Pathologica. 2021;113(3):203-217.

Reyes AC, Egwu E, Yu E, Sanchez AN, De La OL, Elijah OE, et al. Forkhead transcription factor O1 (FoxO1) in torafugu pufferfish Takifugu rubripes: Molecular cloning, in vitro DNA binding, and target gene screening in fish metagenome. Gene. 2021;768:145335.

Shi H, Fang R, Li Y, Li L, Zhang W, Wang H, et al. The oncoprotein HBXIP suppresses gluconeogenesis through modulating PCK1 to enhance the growth of hepatoma cells. Cancer Lett. 2016;382(2):147-156.

Sidali S, Trepo E, Sutter O, Nault J C. New concepts in the treatment of hepatocellular carcinoma. United European Gastroenterol J. 2022;10(7):65-774.

Van Renne N, Roca Suarez AA, Duong FHT, Gondeau C, Calabrese D, Fontaine N, et al. miR-135a-5p-mediated downregulation of protein tyrosine phosphatase receptor delta is a candidate driver of HCV-associated hepatocarcinogenesis. Gut. 2018;67(5):953-962.

Wang S, Xu M, Sun Z, Yu X, Deng Y, Chang H. LINC01018 confers a novel tumor suppressor role in hepatocellular carcinoma through sponging microRNA-182-5p. Am J Physiol Gastrointest Liver Physiol. 2019;317(2):G116-G126.

Wei X, Yang X, Wang B, Yang Y, Fang Z, Yi C, et al. LncRNA MBNL1-AS1 represses cell proliferation and enhances cell apoptosis via targeting miR-135a-5p/PHLPP2/FOXO1 axis in bladder cancer. Cancer Med. 2020;9(2):724-736.

Wei XC, Xia YR, Zhou P, Xue X, Ding S, Liu LJ, et al. Hepatitis B core antigen modulates exosomal miR-135a to target vesicle-associated membrane protein 2 promoting chemoresistance in hepatocellular carcinoma. World J Gastroenterol. 2021;27(48):8302-8322.

Xu JJ, Zheng WH, Wang J, Chen YY. Long non-coding RNA plasmacytoma variant translocation 1 linked to hypoxia-induced cardiomyocyte injury of H9c2 cells by targeting miR-135a-5p/forkhead box O1 axis. Chin Med J (Engl). 2020;133(24):2953-2962.

Xu X, Tao Y, Shan L, Chen R, Jiang H, Qian Z, et al. The Role of MicroRNAs in Hepatocellular Carcinoma. J Cancer. 2018;9(19):3557-3569.

Yan LH, Chen ZN, Li L, Chen J, Wei WE, Mo XW, et al. miR-135a promotes gastric cancer progression and resistance to oxaliplatin. Oncotarget. 2016;43:70699-70714.

Yang C, Huang X, Liu Z, Qin W, Wang C. Metabolism-associated molecular classification of hepatocellular carcinoma. Mol Oncol. 2020;14(4):896-913.

Yang N, Zhou J, Li Q, Han F, Yu Z. miR-96 exerts carcinogenic effect by activating AKT/GSK-3beta/beta-catenin signaling pathway through targeting inhibition of FOXO1 in hepatocellular carcinoma. Cancer Cell Int. 2019;19:38.

Yang S, Pang L, Dai W, Wu S, Ren T, Duan Y, et al. Role of Forkhead Box O Proteins in Hepatocellular Carcinoma Biology and Progression (Review). Front Oncol. 2021;11:667730.

Yao S, Tian C, Ding Y, Ye Q, Gao Y, Yang N, et al. Down-regulation of Kruppel-like factor-4 by microRNA-135a-5p promotes proliferation and metastasis in hepatocellular carcinoma by transforming growth factor-beta1. Oncotarget. 2016;7(27):42566-42578.

Zeng YB, Liang XH, Zhang GX, Jiang N, Zhang T, Huang JY, et al. miRNA-135a promotes hepatocellular carcinoma cell migration and invasion by targeting forkhead box O1. Cancer Cell Int. 2016;16:63.

Zhang CH, Cheng Y, Zhang S, Fan J, Gao Q. Changing epidemiology of hepatocellular carcinoma in Asia. Liver Int. 2022;42(9):2029-2041.

Received for publication on 02nd November 2023
Accepted for publication on 14th March 2024